Dynamic Terahertz Spoof Surface Plasmon–Polariton Switch Based on Resonance and Absorption

Kyungjun Song and Pinaki Mazumder, *Fellow, IEEE*

***Abstract*—In this brief, a terahertz (THz) switch consisting of perfect conductor metamaterials is demonstrated both theoretically and numerically. Specifically, we build a THz logic block based on waveguide–cavity–waveguide, thus providing a strong electromagnetic field accumulation inside a small cavity. Furthermore, this brief shows that the subwavelength metallic cavity can confine light for a long time within a very small area. Therefore, an arbitrarily designed cavity with the high quality factor Q and the small effective area $A_{\rm eff}$ can be easily utilized for an efficient THz switch. These promising results can be used to provide new switch types and open up new vistas in the area of THz subwavelength optics.**

***Index Terms*—Absorption, cavity, dynamic circuit, filter, resonance, spoof surface plasmon–polariton (SSPP), subwavelength, terahertz (THz).**

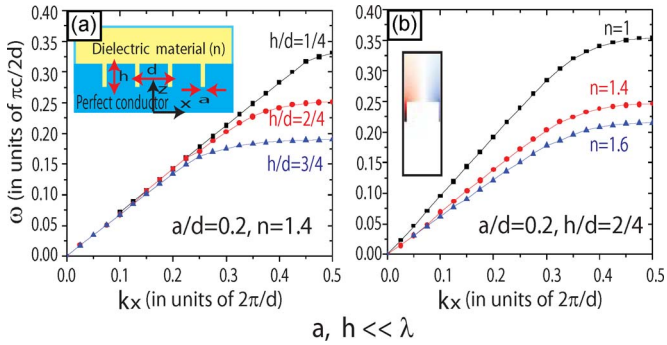

Fig. 1. TM dispersion relationships for SSPP modes are calculated by (a) changing height h and (b) varying the refractive index n.

I. Introduction

RECENTLY, there has been significant interest in developing subwavelength terahertz (THz) pulse propagation through the use of grooves, holes, and dimples created on the surface of metallic structures [1]–[5]. Specifically, a 1-D corrugated metallic structure provides spoof surface plasmon–polariton (SSPP) localization and slow-light propagation when the operational frequency is close to the band edge. Furthermore, transverse magnetic (TM) SSPP modes can be easily modulated by varying height h, as shown in Fig. 1(a), thus providing efficient passive THz elements such as guiding structures, focusing elements, and filters [1]–[5]. In addition, the dynamic control of SSPP modes can be achieved by altering the refractive index n, as illustrated in Fig. 1(b), thereby yielding the feasibility of dynamic THz elements such as switches, modulators, and multiplexers [6].

However, to increase the slow down factor $S = v_c/v_g$, which is defined as the ratio of phase velocity and group velocity, and utilize passband and stop-band characteristics similar to photonic crystals, we use subwavelength metallic gap structures with a periodic array of grooves. Specifically, resonant modes exist within the second band, thus providing a low group velocity, a small damping coefficient, and strong SSPP confinement. Furthermore, the promising capability of SSPP modes is the miniaturization of THz elements and devices on subwavelength scale, which is expected to spur the development of compact, ultrafast, and low-power digital THz circuitry.

In [6], we demonstrated how a metamaterial corrugated structure consisting of a perfect metal and an anisotropic dielectric composed of electrooptically controllable refractive index materials such as a nematic liquid crystal (LC) can be utilized to build dynamically controllable switching waveguides. Nonetheless, significant challenges need to be resolved before THz Boolean circuitry designs can be used to usher in THz information processing. For example, a distributed electrooptic voltage needs to be applied along the length of the LC dielectric, so that the LC is uniformly polarized. In addition, the switching speed of the LC is currently significantly slower than a THz SSPP signal, thereby limiting the application of the switch to merely programmable waveguide networks.

In order to overcome these critical limitations, we propose a THz switch design that involves modifications to the height of the corrugated structure along the length of the waveguide. The idea is to create a small narrow cavity connected to identical waveguides on both sides, as shown in Fig. 2(a). The cavity, which was made up of a small periodic unit cell array, was designed carefully in order to solve the size issue of the switching junction. Furthermore, the switching junction designed using the high quality factor Q and the small effective area $A_{\rm eff}$ enables us to obtain an efficient THz switching function at the small refractive index modulation $\delta n/n$ and the loss-induced modulation $\delta\alpha$.

Manuscript received November 6, 2010; revised March 20, 2011; accepted March 21, 2011. Date of publication May 12, 2011; date of current version June 22, 2011. This work was supported in part by the Air Force Office of Scientific Research under Grant FA9950-06-1-0493. The review of this brief was arranged by Editor A. Schenk.

The authors are with the University of Michigan, Ann Arbor, MI 48109 USA (e-mail: songk@umich.edu; mazum@eecs.umich.edu).

Color versions of one or more of the figures in this brief are available online at http://ieeexplore.ieee.org.

Digital Object Identifier 10.1109/TED.2011.2135370

0018-9383/$26.00 © 2011 IEEE

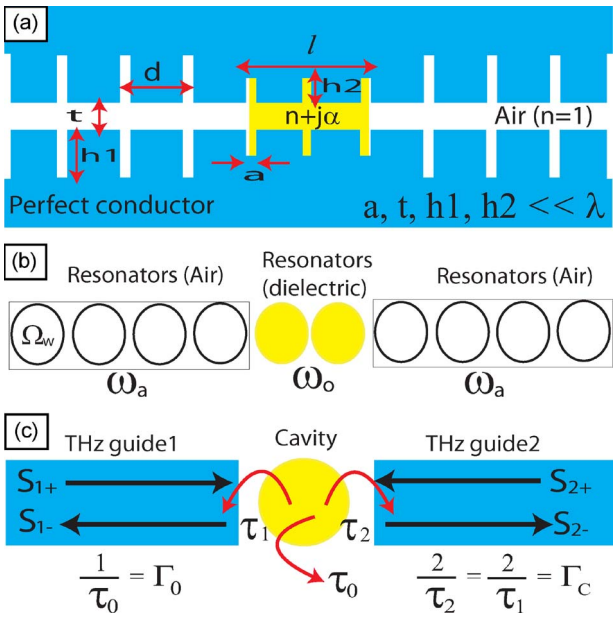

Fig. 2. (a) THz waveguide–cavity–waveguide with 1-D periodicity. (b) THz waveguide can be regarded as a large resonator array with free space ($n = 1$), and the cavity can be considered as a small resonator array with the different height h and the refractive index n. (c) Schematic diagram illustrating the essential physics used in the THz filters and switches.

II. Design of the THz SSPP Waveguide and the Cavity

In this brief, we focus on the waveguide–cavity–waveguide structure for THz filters or switches, where an example of which is shown in Fig. 2(a) [7]–[10]. As shown in Fig. 2(b), the THz waveguides can be considered as equal-space coupled resonator arrays with the single-cavity resonant frequency Ω_W, thus providing the maximum field concentration at the specific frequency ω_a behaving like a THz filter. In addition, a small resonator array with the different height h and the refractive index n can be regarded as a cavity with the resonant frequency ω_o. Because the cavity is formed by reducing the height of the corrugated structure adjacent to the THz waveguides, there are three main physical mechanisms to determine the ON–OFF switching function: by tuning the resonant frequency ω_o, the waveguide–cavity coupling rate Γ_c, and the intrinsic cavity decay rate Γ_o, as shown in Fig. 2(c) [11], [12].

First, we consider the SSPP dispersion of THz waveguides consisting of two sandwiched SSPP gap structures with geometrical parameters of $a/d = 0.1$, $h1/d = 0.8$, $t/d = 1/3$, $d = 100$ μm, and $n = 1$, as shown in Fig. 3(a). We use the air waveguides of $n = 1$ rather than the dielectric waveguides of $n > 1$ to eliminate inherent loss inside the THz waveguides. The SSPP dispersion curves of these structures show multiple SSPP-confined modes, thus providing photonic bandgap management. In addition, we conduct a finite-element method (FEM) simulation, as shown in Fig. 3(b), to verify the THz signal propagation along the corrugated sandwiched metamaterial structure. For instance, the frequency lies in the vicinity of the first band edge at 0.72 THz, thus generating a relatively strong SSPP confinement. However, at 0.9 THz, the frequency is located at the photonic bandgap region, thus prohibiting THz

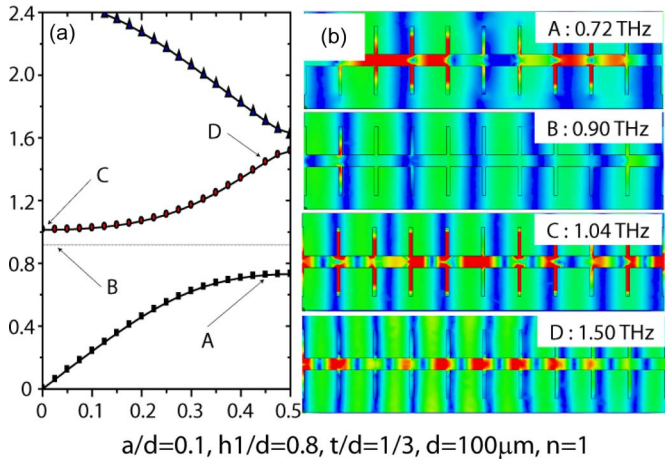

Fig. 3. (a) TM dispersion curves of SSPP modes supported by the sandwiched metamaterial conductor with geometrical parameters of $d = 100$ μm, $a = 10$ μm, $h = 80$ μm, $t = 100/3$ μm, and $n = 1$. (b) Finite-element simulation. Spatial distributions of the electromagnetic field (e-field) across the THz waveguides for four different frequencies of 0.72, 0.9, 1.04, and 1.5 THz, respectively. To explain the theoretical concept, we conducted a FEM simulation based on a 3-D architecture with open sides (width = 500 μm from the y-direction). Because of a large width, there are negligible differences between 3-D and 2-D simulations.

signal propagation. As we increase to 1.04 THz, the THz signals are strongly localized at the grooves within the sandwiched structure, thus realizing slow light propagation along the periodic gap structure. If we increase the frequency up to 1.5 THz, the THz signals provide small localization, as shown in Fig. 3(b). Therefore, the operational frequency of our device is 1.04 THz with λ of $\sim$288 μm. At the given frequency, the THz design parameters have metamaterial conditions of $a = \sim\lambda/30$ and $t = \sim\lambda/9$, in contrast with conventional metallic grating waveguides [13], [14].

Next, we introduce linear localization with a grating period of $N = 2$ into the background THz filters by reducing the height of the THz structure, as shown in Fig. 2(a). To obtain efficient transmission across the THz filter, it is essential that both the resonant frequency ω_o of the cavity and the specific frequency ω_a of THz waveguides coincide, as demonstrated in Fig. 2(b). Furthermore, the resonant frequency of SSPP modes is almost inversely proportional to height h and the refractive index n; therefore, the height of the cavity structure with the dielectric material $(n > 1)$ should be smaller than the THz waveguides. Specifically, we designed a cavity structure with geometrical parameters of $l = 2d$, $a/d = 0.1$, $t/d = 1/3$, $h2/d = 0.5$, and $n = 1.414$, as shown in Fig. 2(a). With these conditions, we obtain a resonant frequency ω_o value of $\sim 1.38\pi c/2d$ with a Q factor of $\sim$690 using the finite-difference time-domain method (FDTD).

III. SSPP Switching Based on Resonance

We designed a narrow SSPP bandpass filter with a waveguide–cavity–waveguide structure. Next, we will consider how this structure can be extended to dynamic THz switches. In principle, as n increases, ω_o shifts to a lower frequency. In contrast, as n decreases, ω_o moves to a higher frequency. For example, let us assume that the intrinsic cavity decay rate

Γ_o is negligible; thus, $\Gamma_o \to 0$. The transmission and reflection can then be described using temporal coupled-wave analysis (TCWA) [15], [16] as follows:

$$T(\omega) = \frac{(\Gamma_c)^2}{(\omega-\omega_0)^2+(\Gamma_c)^2} \text{ and } R(\omega) = \frac{(\omega-\omega_0)^2}{(\omega-\omega_0)^2+(\Gamma_c)^2}. \quad (1)$$

Specifically, (1) leads to two fundamental limiting switching conditions. In one case, $|\omega-\omega_o| = \Delta\omega_o \ll \Gamma_c$. Equation (1) illustrates that almost all power from waveguide 1 can be transferred to waveguide 2, thus demonstrating an ON-state. For the opposite case, $|\omega-\omega_o| = \Delta\omega_o \gg \Gamma_c$. The frequency of the SSPP mode has a large shift from the resonant frequency ω_o. The reflection almost approaches unity, thus achieving an OFF-state.

Specifically, we obtain $\Delta\omega_o$ of $\sim 0.0104\pi c/2d$ at $\delta n = 0.01$ by using the SSPP dispersion analysis. Next, Γ_c can be obtained by

$$\Gamma_c = \frac{\omega_o}{2Q} \sim \frac{(1-R)v_g}{L_{\text{cav}}}. \quad (2)$$

The FDTD simulation yields a Q factor of $\sim$690 within the cavity structure with length $L_{\text{cav}} = 2d$, thus providing $\Gamma_c = 0.001015\pi c/2d$. Therefore, the switching function can be realized by modulating the refractive index at $\delta n/n = 0.01$ due to $\Gamma_c \ll \Delta\omega_o$. As shown in (2), Γ_c can be determined by the group velocity ν_g and the reflective coefficient R of the cavity. Thus, the ON-OFF switching ratio can be enhanced if we create slow-light waves and high-reflection structures. Therefore, it is essential to consider optimal switching when building an efficient THz switch constrained by two fundamental cavity parameters, i.e., a Q factor inversely proportional to the decay rate of a cavity photon and the small effective volume V_{eff} determining the photon intensity inside the cavity [17].

First, a high Q factor is needed to decrease Γ_c and increase the switching function at small $\delta n/n$, as provided in (2). For example, we can design the cavity structure by placing the blocking structures, as shown in the inset in Fig. 4(a). The Q factor increases correspondingly to the small gap size of the blocking structures as the increased potential barriers of the cavity allow a small energy leakage from the cavity to the waveguides. Thus, the switching functionality can be elevated if we construct cavity structures with a high Q factor, as shown in the inset in Fig. 4(a). To confirm the THz switching using the refractive index modulation, we used the FEM, as shown in Fig. 4(a). As shown, the resonant mode of a cavity $(n = 1.421)$ with no gap $(g = t)$ allows us to achieve almost 100% transmission, which indicates an ON-state. The small difference in resonant frequency between the FDTD method and the FEM originates from numerical noise. Furthermore, the ON–OFF function can be enhanced using high Q design structures ($w = 0.2d$ and $g = d/12$), thereby yielding a 3-dB switching extinction ratio at a $\delta n/n$ value of $\sim$0.002.

However, the intrinsic losses in the metal affect the Q factors in the cavity, thus limiting the switching performance. For example, we use Ag properties with a conductivity value of

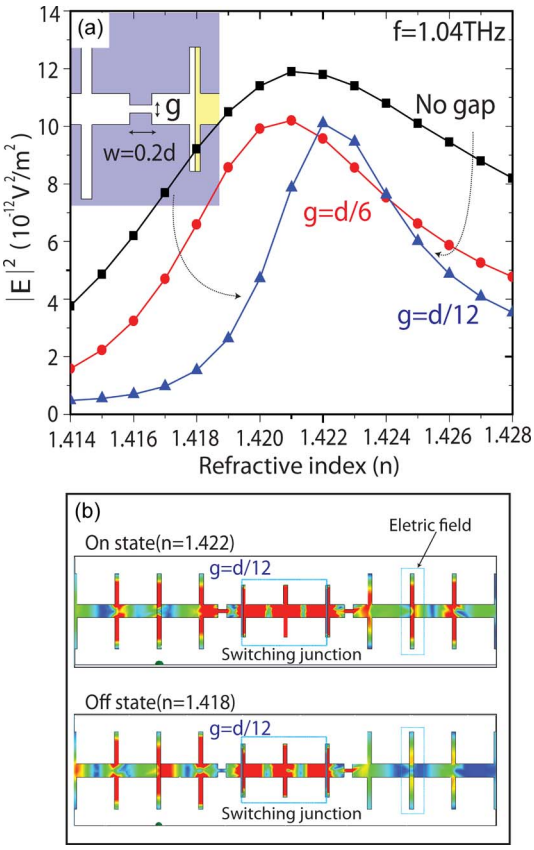

Fig. 4. (a) The magnitude of an e-field of $f = 1.04$ THz in a metallic groove located at 800 μm, corresponding to the refractive index modulation inside the switching junction. The THz waveguides and cavity have the same geometrical parameters, as shown in Fig. 3. The blocking structures have geometrical parameters of $w = 0.2d$ and $g = d/3$, $d/6$, and $d/12$, respectively. (b) Spatial snapshots of the e-field show an ON-state at $n = 1.422$ and an OFF-state at $n = 1.418$, respectively.

$\sigma = 6.1 \times 10^7\ \Omega^{-1}\text{m}^{-1}$. Furthermore, the 3-dB switching extinction ratio of a switch with Ag blocking structures of $w = 0.2d$ and $g = d/12$ can be achieved at a $\delta n/n$ value of $\sim$0.007 through FEM simulation.

As an alternative method, we can increase the energy accumulation inside the cavity if we decrease the size of the switching junction area A_{eff}, as shown in the inset in Fig. 5. As expected, a switching junction with a small dimension requires a large refractive index of $n = 1.961$ for its resonant frequency. Although a size reduction induces a small propagation length due to the large potential barriers between the cavity and waveguides, this structure allows us to obtain a 3-dB switching extinction ratio at a $\delta n/n$ value of $\sim$0.0025, thus demonstrating the usefulness of energy accumulation for switching functionality.

IV. SSPP Switching Based on Absorption

As a different approach, absorption modulation can be considered as a new method for THz signal control and routing. To verify loss-induced THz switching, let us now turn to the case of purely absorptive modulation, in which the input field frequency ω coincides with both the cavity resonance ω_o and

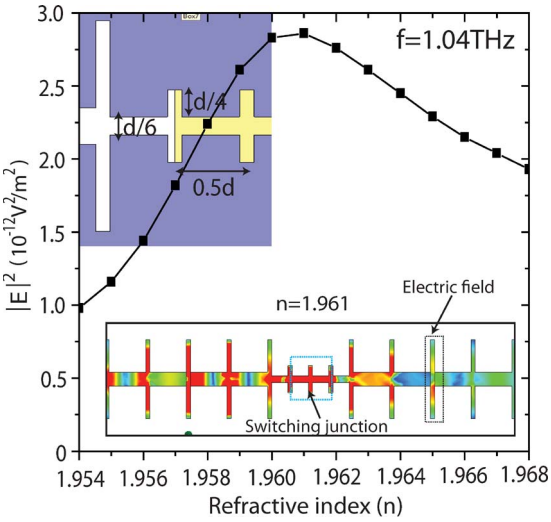

Fig. 5. Magnitude of an e-field of $f = 1.04$ THz in a metallic groove located at 800 μm, corresponding to the refractive index modulation inside the switching junction. THz waveguides have the same geometrical parameters shown in Fig. 4. In addition, the cavity has geometrical parameters of $d = 50$ μm, $a = 10$ μm, $h = 25$ μm, and $t = 100/6$ μm.

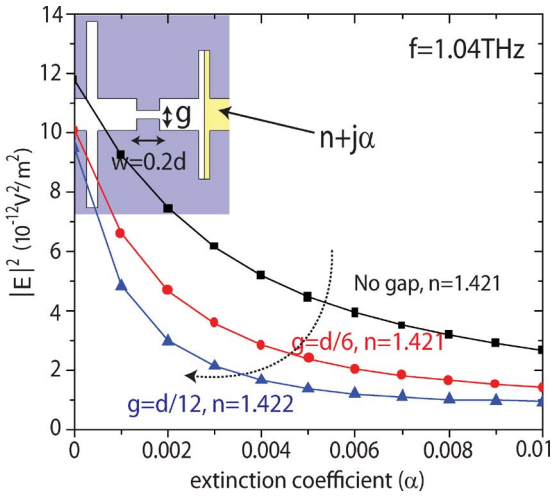

Fig. 6. Magnitude of an e-field of $f = 1.04$ THz in a metallic groove located at 800 μm corresponding to the extinction coefficient α inside the switching junction. All geometrical configurations are the same as those in Fig. 4.

the specific frequency ω_a of the waveguides. Thus, TCWA gives the following:

$$T(\omega) = \frac{(\Gamma_c)^2}{(\Gamma_c + \Gamma_o)^2} \quad \text{and} \quad R(\omega) = \frac{(\Gamma_o)^2}{(\Gamma_c + \Gamma_o)^2}. \quad (3)$$

The only dependent parameters for determining transmission and reflection are Γ_o and Γ_c. More specifically, we consider two fundamental limiting cases: In the first case, $\Gamma_o \ll \Gamma_c$, and the switching state is on. In the second case, $\Gamma_c \ll \Gamma_o$, and the switching state is off. As such, we assume that Γ_o only depends on the extinction coefficient α of the dielectric material inside the cavity. Hence, Γ_o can be approximately given by a Γ_o value of $\sim 2\omega\alpha/n$ with a dielectric material permittivity value of $\varepsilon = (n + j\alpha)^2$. At a resonant frequency ω_o value of $\sim 1.38\pi c/2d$, where $n = 1.421$ and $\alpha = 0.01$, the intrinsic cavity decay rate is almost equal to a Γ_o value of $\sim 0.0194\pi c/2d$, which means $\Gamma_o \gg \Gamma_c$ (i.e., Q is $\sim$690, and $\Gamma_c = 0.001015\pi c/2d$); thus, $T(\omega)$ is $\sim$0 and $R(\omega)$ is $\sim$1, as provided in (3). The FEM simulation validates THz switching using the loss-induced method. As illustrated in Fig. 6, the inherent loss-free systems yield an ON-state from a resonant matching condition of $\omega = \omega_a = \omega_o$. On the other hand, as α increases, the output power is significantly reduced, as expected in (3). Similar to the resonance modulation, a high Q factor is useful for obtaining a switching function at a small $\delta\alpha$ value. For example, a switch with blocking structures of $w = 0.2d$ and $g = d/12$ allows us to obtain a 3-dB extinction ratio at a $\delta\alpha$ value of $\sim$0.0015.

V. Conclusion

In this brief, we focused on THz switches using subwavelength channels composed of perfect conductor metamaterials based on resonance and absorption. In addition, dielectric materials such as n-GaAS or SI-GaAS are possible candidates for THz switching. Similarly, dynamic THz switching can be achieved using GaAS [18]. However, the performance of SSPP devices is highly robust against fluctuations in geometrical or material parameters due to a subwavelength tunneling mechanism t value of $\sim\lambda/9$. In addition, we note that, although a high Q factor is desirable for an ON–OFF switching function, it is essential to consider resonant matching issues ($\omega = \omega_a = \omega_o$) resulting from a small bandwidth.

Nevertheless, we expect that the proposed idea can be implemented to future THz devices such as Mach–Zehnder interferometers, amplifiers, nonlinear switches, and biosensors. Furthermore, SSPP architectures can be applied to slow-light devices operating at radio-to-microwave frequencies.

References

[1] J. B. Pendry, L. Martín-Moreno, and F. J. Garcia-Vidal, "Mimicking surface plasmons with structured surfaces," *Science*, vol. 305, no. 5685, pp. 847–848, Aug. 2004.

[2] S. A. Maier, S. R. Andrews, L. Martín-Moreno, and F. J. García-Vidal, "Terahertz surface plasmon–polariton propagation and focusing on periodically corrugated metal wires," *Phys. Rev. Lett.*, vol. 97, no. 17, p. 176 805, Oct. 2006.

[3] A. P. Hibbins, B. R. Evans, and J. R. Sambles, "Experimental verification of designer surface plasmons," *Science*, vol. 308, no. 5722, pp. 670–672, Apr. 29, 2005.

[4] S. A. Maier and S. R. Andrews, "Terahertz pulse propagation using plasmon–polariton-like surface modes on structured conductive surfaces," *Appl. Phys. Lett.*, vol. 88, no. 25, p. 251 120, Jun. 2006.

[5] A. I. Fernandez-Dominguez, L. Martin-Moreno, F. J. Garcia-Vidal, S. R. Andrews, and S. A. Maier, "Spoof surface plasmon polariton modes propagating along periodically corrugated wires," *IEEE J. Sel. Topics Quantum Electron.*, vol. 14, no. 6, pp. 1515–1521, Nov./Dec. 2008.

[6] K. Song and P. Mazumder, "Active terahertz spoof surface plasmon polariton switch comprising the perfect conductor metamaterial," *IEEE Trans. Electron Devices*, vol. 56, no. 11, pp. 2792–2799, Nov. 2009.

[7] M. Nagel and H. Kurz, "Corrugated waveguide based genomic biochip for marker-free THz read-out," *Int. J. Infrared Millim. Waves*, vol. 27, no. 4, pp. 517–529, Apr. 2006.

[8] M. Gerhard, C. Imhof, and R. Zengerle, "Compact three-dimensional terahertz resonators based on periodically corrugated metallic slit waveguides," *J. Appl. Phys.*, vol. 108, no. 2, p. 026 102, Jul. 2010.

[9] S. S. Harsha, N. Laman, and D. Grischkowsky, "High-Q terahertz Bragg resonances within a metal parallel plate waveguide," *Appl. Phys. Lett.*, vol. 94, no. 9, p. 091 118, Mar. 2009.

[10] M. Nagel, P. Haring Bolivar, and H. Kurz, "Modular parallel-plate THz components for cost-efficient biosensing systems," *Semicond. Sci. Technol.*, vol. 20, no. 7, pp. S281–S285, Jul. 2005.

[11] S. Fan and J. D. Joannopoulos, "Analysis of guided resonances in photonic crystal slabs," *Phys. Rev. B, Condens. Matter*, vol. 65, no. 23, p. 235 112, Jun. 2002.
[12] Y. Xu, Y. Li, R. K. Lee, and A. Yariv, "Scattering-theory analysis of waveguide–resonator coupling," *Phys. Rev. E, Stat. Phys. Plasmas Fluids Relat. Interdiscip. Top.*, vol. 62, no. 5, pp. 7389–7404, Nov. 2000.
[13] B. D. McVey, M. A. Basten, J. H. Booske, J. Joe, and J. E. Scharer, "Analysis of rectangular waveguide-gratings for amplifier applications," *IEEE Trans. Microw. Theory Tech.*, vol. 42, no. 6, pp. 995–1003, Jun. 1994.
[14] G. I. Zaginaylov, A. Hirata, T. Ueda, and T. Shiozawa, "Full-wave modal analysis of the rectangular waveguide grating," *IEEE Trans. Plasma Sci.*, vol. 28, no. 3, pp. 614–620, Jun. 2000.
[15] W. Suh, Z. Wang, and S. Fan, "Temporal coupled-mode theory and the presence of non-orthogonal modes in lossless multimode cavities," *IEEE J. Quantum Electron.*, vol. 40, no. 10, pp. 1511–1518, Oct. 2004.
[16] S. H. Fan, W. Suh, and J. D. Joannopoulos, "Temporal coupled-mode theory for the Fano resonance in optical resonators," *J. Opt. Soc. Amer. A, Opt. Image Sci. Vis.*, vol. 20, no. 3, pp. 569–572, Mar. 2003.
[17] K. J. Vahala, "Optical microcavities," *Nature*, vol. 424, no. 6950, pp. 839–846, Aug. 2003.
[18] H.-T. Chen, W. J. Padilla, J. M. O. Zide, A. C. Gossard, A. J. Taylor, and R. D. Averitt, "Active terahertz metamaterial devices," *Nature*, vol. 444, no. 7119, pp. 597–600, Nov. 2006.

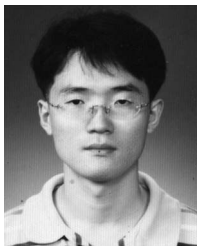

Kyungjun Song received the Ph.D. from the University of Michigan, Ann Arbor, in 2010.

He is currently a Postdoc with the Department of Electrical Engineering and Computer Science, University of Michigan. His research interests include modeling, simulation, and design of plasmonic nanoarchitecture.

Pinaki Mazumder (F'99) received the Ph.D. degree from the University of Illinois at Urbana-Champaign, Urbana-Champaign, in 1988.

He had worked for six years in industrial research and development centers, which included AT&T Bell Laboratories, where he started in 1985 the CONES Project, which is the first C modeling-based very-large-scale-integration (VLSI) synthesis tool, and India's premiere electronics company Bharat Electronics Ltd., where he had developed several high-speed and high-voltage analog integrated circuits intended for consumer electronics products. Currently, he is a Professor with the Department of Electrical Engineering and Computer Science, University of Michigan, Ann Arbor. He has published over 200 technical papers and four books on various aspects of VLSI research works. His research interests include current problems in nanoscale complementary metal-oxide-semiconductor (CMOS) VLSI design, computer-aided design tools and circuit designs for emerging technologies including quantum MOS and resonant tunneling devices, semiconductor memory systems, and physical synthesis of VLSI chips.

Dr. Mazumder was a recipient of Digital's Incentives for Excellence Award, the BF Goodrich National Collegiate Invention Award, and the Defense Advanced Research Projects Agency Research Excellence Award. He is an American Association for the Advancement of Science Fellow (2008) for his contributions to the field of VLSI.